



**HAL**  
open science

## Accumulation of propionic acid during consecutive batch anaerobic digestion of commercial food waste

Gabriel Capson-Tojo, Diane Ruiz, Maxime Rouez, Marion Crest, Jean-Philippe Steyer, Nicolas Bernet, Jean-Philippe Delgenès, Renaud Escudié

### ► To cite this version:

Gabriel Capson-Tojo, Diane Ruiz, Maxime Rouez, Marion Crest, Jean-Philippe Steyer, et al.. Accumulation of propionic acid during consecutive batch anaerobic digestion of commercial food waste. *Bioresource Technology*, 2017, 245, pp.724-733. 10.1016/j.biortech.2017.08.149 . hal-04180656

**HAL Id: hal-04180656**

**<https://hal.inrae.fr/hal-04180656>**

Submitted on 13 Aug 2023

**HAL** is a multi-disciplinary open access archive for the deposit and dissemination of scientific research documents, whether they are published or not. The documents may come from teaching and research institutions in France or abroad, or from public or private research centers.

L'archive ouverte pluridisciplinaire **HAL**, est destinée au dépôt et à la diffusion de documents scientifiques de niveau recherche, publiés ou non, émanant des établissements d'enseignement et de recherche français ou étrangers, des laboratoires publics ou privés.



Distributed under a Creative Commons Attribution - NonCommercial - NoDerivatives 4.0 International License

## Accepted Manuscript

Accumulation of propionic acid during consecutive batch anaerobic digestion of commercial food waste

Gabriel Capson-Tojo, Diane Ruiz, Maxime Rouez, Marion Crest, Jean-Philippe Steyer, Nicolas Bernet, Jean-Philippe Delgenès, Renaud Escudié

PII: S0960-8524(17)31463-3  
DOI: <http://dx.doi.org/10.1016/j.biortech.2017.08.149>  
Reference: BITE 18758

To appear in: *Bioresource Technology*

Received Date: 29 June 2017  
Revised Date: 22 August 2017  
Accepted Date: 23 August 2017

Please cite this article as: Capson-Tojo, G., Ruiz, D., Rouez, M., Crest, M., Steyer, J-P., Bernet, N., Delgenès, J-P., Escudié, R., Accumulation of propionic acid during consecutive batch anaerobic digestion of commercial food waste, *Bioresource Technology* (2017), doi: <http://dx.doi.org/10.1016/j.biortech.2017.08.149>

This is a PDF file of an unedited manuscript that has been accepted for publication. As a service to our customers we are providing this early version of the manuscript. The manuscript will undergo copyediting, typesetting, and review of the resulting proof before it is published in its final form. Please note that during the production process errors may be discovered which could affect the content, and all legal disclaimers that apply to the journal pertain.



## Accumulation of propionic acid during consecutive batch anaerobic digestion of commercial food waste

Gabriel Capson-Tojo <sup>a,b</sup>, Diane Ruiz <sup>a</sup>, Maxime Rouez <sup>b</sup>, Marion Crest <sup>b</sup>, Jean-Philippe Steyer <sup>a</sup>, Nicolas Bernet <sup>a</sup>, Jean-Philippe Delgenès <sup>a</sup>, Renaud Escudie <sup>a,\*</sup>

<sup>a</sup> LBE, INRA, Univ. Montpellier, 102 avenue des Etangs, 11100, Narbonne, France

<sup>b</sup> Suez, CIRSEE, 38 rue du Président Wilson, 78230, Le Pecq, France

\* Corresponding author: tel. +33 (0) 468.425.173, e-mail: [renaud.escudie@inra.fr](mailto:renaud.escudie@inra.fr)

### Abstract

The objective of this study was to test three different alternatives to mitigate the destabilizing effect of accumulation of ammonia and volatile fatty acids during food waste anaerobic digestion. The three options tested (low temperature, co-digestion with paper waste and trace elements addition) were compared using consecutive batch reactors. Although methane was produced efficiently ( $\sim 500 \text{ mlCH}_4 \cdot \text{gVS}^{-1}$ ;  $16 \text{ lCH}_4 \cdot \text{l reactor}^{-1}$ ), the concentrations of propionic acid increased gradually (up to  $21.6 \text{ g} \cdot \text{l}^{-1}$ ). This caused lag phases in the methane production and eventually led to acidification at high substrate loads. The addition of trace elements improved the kinetics and allowed higher substrate loads, but could not avoid propionate accumulation. Here, it is shown for the first time that addition of activated carbon, trace elements and dilution can favor propionic acid consumption after its accumulation. These promising options should be optimized to prevent propionate accumulation.

### Keywords

Biomethane; characterization; acidification; granular activated carbon

## 1. Introduction

Moving our society towards a circular economy and a sustainable future, food waste (FW) must be considered as a resource. In addition, the European Directive 2008/98/CE imposes the valorization of commercial FW from large producers through soil return. Among all the options for FW valorization, anaerobic digestion (AD) allows the conversion of organic matter into biogas and digestate. Considering FW as a substrate for AD, it has been stated that these two end-products may have huge implications for production of renewable energy (Thi et al., 2016) and for recovery of nutrients (Stoknes et al., 2016), respectively. Moreover, the benefits of AD when compared to other treatment methods, such as landfilling, incineration or composting have been previously proved (Bernstad et al., 2016).

However, AD of FW is a complex process associated with several issues. In short term, as FW is mainly composed of easily degradable carbohydrates, reactor overloading and initial accumulation of volatile fatty acids (VFAs) have been frequently reported due to unbalance of the acidogenesis/acetogenesis and methanogenesis steps (Capson-Tojo et al., 2016). In addition, during long term operation several authors have reported high concentrations of total ammonia nitrogen (TAN) and thus free ammonia nitrogen (FAN), which is toxic to microorganisms (Banks et al., 2008; Rajagopal et al., 2013). This occurs due to the high protein content of FW. Proteins are rich in organic N, which is reduced to TAN during AD. The high TAN concentrations achieved during AD of FW have been found to be responsible for inhibiting acetoclastic methanogens, which are known to be more sensitive to high TAN/FAN concentrations (inhibited over  $2.8\text{-}3.0\text{ g TAN}\cdot\text{l}^{-1}$ ) than hydrogenotrophic/mixotrophic archaea (De Vrieze et al., 2012). Thus, this latter archaea are the predominant species at the high TAN concentrations associated with FW AD (Jiang et al., 2017). As a conclusion, different studies have suggested that syntrophic acetate oxidation

(SAO) and hydrogenotrophic methanogenesis (HM) are predominant pathways for methane production during AD of FW (Banks et al., 2012; Capson-Tojo et al., 2017; Yirong et al., 2015). In these systems, syntrophic interactions between different groups of bacteria and archaea are particularly important to avoid accumulation of intermediate metabolites such as VFAs, molecular hydrogen or formate. If any of the aforementioned compounds start to build-up in the reactors, it eventually causes acidification of the AD process, decreasing the pH down to values at which the production of methane no longer occurs. Thus, accumulation of VFAs during FW AD has been reported by several authors, causing inefficient AD and eventually process failure (Banks et al., 2008; Wanqin Zhang et al., 2015).

Different options have been proposed to overcome this issue. Among them, co-digestion (*i.e.* simultaneous digestion of two or more substrates) and supplementation of trace elements (TEs) are among the most promising alternatives for achieving stable FW AD (Capson-Tojo et al., 2016). Several co-substrates have been co-digested with FW, such as green waste (X. Chen et al., 2014), manure (Ebner et al., 2016), sludge (Kim et al., 2017), macroalgae (Cogan and Antizar-Ladislao, 2016) or cardboard/paper waste (Asato et al., 2016; Capson-Tojo et al., 2017; Kim and Oh, 2011). Among those co-substrates, lignocellulosic-rich organic matter appears as a convenient option due to their much slower hydrolysis rates when compared with FW (reducing the risk of initial VFA accumulation), their high C/N ratio (diluting N concentrations) and their higher alkalinity. Paper/cardboard waste (PW) is particularly suitable for centralized commercial FW co-digestion, mainly because both wastes are usually the main organic solid waste streams in urban areas (Kim and Oh, 2011; Zhang et al., 2012). Other than co-digestion, the supplementation of TEs has also been found to stabilize AD of FW (Banks et al., 2012; Zhang and Jahng, 2012; Wanli Zhang et al., 2015a). As the results by Banks et al. (2012) suggest, a lack of TEs exists during AD of FW because of the requirements for synthesis of the enzymes needed for syntrophic HM, particularly for the

production of formate dehydrogenase for formate cleavage. In their study, the build-up or formate and/or hydrogen led to accumulation of propionic acid (HPr) in the reactors, whose degradation is thermodynamically favorable only within a small range of concentrations of these species (Batstone et al., 2002). Different TEs have been found to be required for both mesophilic and thermophilic AD of FW, such as iron, selenium, cobalt, molybdenum, nickel or tungsten (Qiang et al., 2013, 2012; Wanqin Zhang et al., 2015). By adding mixtures of these elements, it has been possible to avoid accumulation of VFAs, even at higher organic loading rates (OLRs) than in the reactors without them (Zhang et al., 2011; Wanli Zhang et al., 2015a; Wanqin Zhang et al., 2015). Some authors have even recovered acidified reactors by TEs supplementation (Qiang et al., 2013, 2012).

Besides their wide industrial applicability, consecutive batch reactors have been barely used for solid FW AD. As these systems allow testing several conditions in parallel, they are particularly convenient for AD studies at laboratory and pilot scale. To the knowledge of the authors, no study has been carried out to compare the aforementioned stabilization options (*i.e.* co-digestion and TEs addition) and their ability to avoid accumulation of VFAs at different substrate loads. Moreover, a simple option to decrease the FAN concentration in the reactors is working at low temperatures, displacing the  $\text{NH}_3\text{-NH}_4^+$  equilibrium towards  $\text{NH}_4^+$  and therefore lowering the impact of  $\text{NH}_3$  inhibition.

The objective of this study was to compare the performance of three options for AD stabilization using pilot-scale consecutive batch reactors: working at low temperatures (30 °C vs. 37 °C), co-digestion of FW with PW and supplementation of TEs. The total solids (TS) contents and the concentrations of VFAs and TAN after each consecutive batch were measured. In addition, the digestate from a pilot reactor was used to test different options for favoring the consumption of the VFAs that had progressively accumulated (mainly HPr). An extensive characterization of commercial FWs from different sources was also carried out.

## 2. Materials and methods

### 2.1. Inoculum and substrate

The inoculum used to start the pilot reactors was collected from an industrial plant digesting different organic streams at high TAN/FAN concentrations ( $5.04 \text{ g TAN}\cdot\text{l}^{-1}$ ;  $0.615 \text{ g FAN}\cdot\text{l}^{-1}$ ). Thus, it was assumed that the microbial population was already adapted to high FAN concentrations, such as those existing during FW AD. The sludge had a TS content of  $5.81\pm 0.02 \%$ , with  $59.13\pm 0.08 \%$  corresponding to volatile solids (VS). Concerning the commercial FW, the waste collection was carried out in the region of the Grand Narbonne, in the south of France. Five different mayor FW producers from the region were used as representative examples of potential FW suppliers: (1) fast food restaurant, (2) restaurant, (3) supermarket, (4) fruit and vegetable supermarket and (5) fruit and vegetable distribution. A proportional mixture (wet weight) of the different FWs was used as substrate for the experiments.

### 2.2. Consecutive batch reactors for stabilization of anaerobic digestion

Four different pilot reactors were run in parallel to test the different strategies for AD stabilization. The particular working conditions are shown in Table 1.

The Control reactor was fed with FW and incubated at  $37 \text{ }^\circ\text{C}$ . The reactor T30 had equivalent working conditions, but was kept at  $30 \text{ }^\circ\text{C}$  to lower the FAN proportions. The Co-PW reactor was operated similarly, but a supplementary amount of PW was added as co-substrate (75 % FW:25 % PW w/w). This co-digestion ratio was selected because similar values have been previously applied successfully in the literature (Kim and Oh, 2011; Zhang et al., 2012) and because this is a proportion similar to the one at which FW and PW are generally found in municipal solid waste (Hogg et al., 2002). The PW used was regular office paper grinded to less than 1 cm ( $92.7 \%$  TS;  $77.6 \%$  VS/TS). During the start-up of this reactor, a small amount

of dried compost was added to the inoculum to increase the initial TS contents to values close to those expected after several consecutive batches using this substrate (around 9 % TS).

Finally, the Sup-TEs reactor had equivalent working conditions to those of the Control reactor but was supplemented with TEs at the following concentrations: 100 mg·l<sup>-1</sup> Fe, 1 mg·l<sup>-1</sup> Co, 5 mg·l<sup>-1</sup> Mo, 5 mg·l<sup>-1</sup> Ni, 0.2 mg·l<sup>-1</sup> Se, 0.2 mg·l<sup>-1</sup> Zn, 0.1 mg·l<sup>-1</sup> Cu, 1 mg·l<sup>-1</sup> Mn. These values were calculated from optimal results reported in the literature (Banks et al., 2012; Zhang and Jahng, 2012; Wanli Zhang et al., 2015a). The required volume of a concentrated solution (x100) containing FeCl<sub>2</sub>·4H<sub>2</sub>O, CoCl<sub>2</sub>·6H<sub>2</sub>O, Na<sub>2</sub>MoO<sub>4</sub>·2H<sub>2</sub>O, NiCl<sub>2</sub>·6H<sub>2</sub>O, Na<sub>2</sub>SeO<sub>3</sub>, ZnCl<sub>2</sub>·2H<sub>2</sub>O, CuCl<sub>2</sub>·2H<sub>2</sub>O, MnCl<sub>2</sub>·4H<sub>2</sub>O was used for doping the reactor.

Concerning the reactor loading, the same procedure was applied in all the systems. The first load was 0.087 kg FW·kg inoculum<sup>-1</sup> (corresponding to an initial substrate to inoculum ratio (S/X) of 0.25 g VS·g VS<sup>-1</sup>), continuing with 0.173 FW·kg inoculum<sup>-1</sup> (two-fold initial load) and 0.260 kg FW·kg inoculum<sup>-1</sup> (three-fold initial load). The reactors were fed when a biogas plateau was reached or when yields of approximately 500 ml CH<sub>4</sub>·g VS<sup>-1</sup> (common biochemical methane potential (BMP) value for FW (Capson-Tojo et al., 2016)) were obtained. When feeding, the required amount of digestate was removed to keep a constant working volume in the reactors. It is important to consider that, as the kinetics of biogas production in the reactors differed, the reactors were not fed at the same times and a different number of feeding cycles was achieved in each condition throughout the operational period.

Table 2 aims to summarize the loading regime applied in the four reactors (*i.e.* Control and three stabilization strategies). The Control reactor and the reactors T30 and Co-PW were started at the first selected load (Cycle 1; 0.087 kg FW·kg inoculum<sup>-1</sup>). It must be mentioned that this first cycle was used for adaptation of the inoculum and therefore the three reactors had the same working conditions (37 °C and FW as substrate; grey-shaded methane yields in Figure 1). The specific conditions of T30 and Co-PW were started in Cycle 2 (with the same

load of Cycle 1). In the 3<sup>rd</sup> cycle, the load was doubled in all the pilots, and the Sup-TEs reactor was started with inoculum issued from the Control reactor and with the same load that was applied in the other pilots (0.173 kg FW·kg inoculum<sup>-1</sup>). This allowed the comparison between the different conditions. To permit a straight-forward comparison between the Control and the Sup-TEs after the start-up of the latter, the first 2 feeding cycles of the Control (used for inoculating Sup-TEs) are also presented in the figure showing the performance on Sup-TEs (grey-shaded methane yields in Figure 1).

The experiments lasted a minimum of 173 days (Co-PW) and a maximum of 187 days (Control). The reactors consisted of cylindrical vessels made of stainless steel that were continuously agitated by inner stirring blades. A more precise description of these reactors can be found elsewhere (Ganesh et al., 2013).

### *2.3. Batch essay for investigating the VFA consumption*

After 159 days of operation, 4 kg of digestate from the Co-PW reactor were sampled and used to test different options for favoring the consumption of the accumulated VFAs. Table 3 summarizes the different working conditions defined.

All these reactors were fed with 288 ml of digestate and incubated at 37 °C for 142 days. The influence on the VFA consumption of the addition of TEs was tested at two different concentrations: (i) the TEs concentration defined previously for the pilot reactor Sup-TEs (corresponding to 100 mg Fe·l<sup>-1</sup>), and (ii) a reactor with a 5-folded concentration (corresponding to 500 mg Fe·l<sup>-1</sup>). The effect of the supplementation of granular activated carbon (GAC; Sigma-Aldrich, Missouri, United States of America; CAS 7440-44-0) was also assessed. Addition of GAC has been reported to favor adsorption of inhibitors, allowing at the same time the formation of biofilms onto its surface, which has been shown to favor syntrophic interactions (Fagbohunge et al., 2017). In addition, GAC allows direct interspecies electron transfer (DIET), avoiding the formation of electron shuttles (such as

hydrogen or formate) and favoring acetic acid (HAc) consumption (Dang et al., 2016; Lee et al., 2016). An initial GAC concentration of  $10 \text{ g}\cdot\text{l}^{-1}$  was selected according to Lee et al. (2016). A last reactor was defined (1/2Dilution) to evaluate the effect on VFA consumption of simply diluting the digestate, aiming to reduce thermodynamic inhibitions. A Control reactor was also defined to perform an un-biased evaluation of the effect of these different options. The reactors used were specifically designed to allow sampling of the digesting medium during the AD process without disturbing the gas in the headspace (Motte et al., 2015). As a consequence, the dynamics of both the biogas production and the VFA consumption-production were followed.

#### *2.4. Analytical methods*

##### *2.4.1. Physicochemical characterization of the commercial FW*

The characterization of commercial FW is a crucial step prior to its valorization. In addition, its characteristics are source dependent. Therefore, an extensive characterization of the commercial FW from the different suppliers was performed. TS and VS contents were measured according to the standard methods of the American Public Health Association (APHA, 2005). The concentration of carbohydrates was measured by the Dubois method (Dubois et al., 1956). The content of lipids was determined by a gravimetric method based on accelerated solvent extraction using an ASE<sup>®</sup>200, DIONEX coupled to a MULTIVAPOR P-12, BUCHI with heptane as solvent (100 bar, 105 °C, 5 cycles of 10 min static and 100s purge) (APHA, 2005). Total Kjeldahl nitrogen (TKN) and  $\text{NH}_4^+$  concentrations were measured with an AutoKjeldahl Unit K-370, BUCHI. The concentration of proteins was estimated from the TKN contents using a conversion factor of  $6.25 \text{ g protein}\cdot\text{g N}^{-1}$  (Jimenez et al., 2013). Total organic carbon (TOC) and inorganic carbon (IC) were determined using a Shimadzu TOC-V<sub>CSN</sub> Total Organic Carbon Analyzer coupled to a Shimadzu ASI-V tube rack. The total carbon (TC) was calculated as the sum of TOC and IC. The pH was measured

by a WTW pHmeter series inoLab pH720. The BMPs of the substrates were determined according to Motte et al. (2014).

The concentrations of micro/macro-elements were measured by Aurea Agrosience<sup>®</sup> (Ardon, France) as follows: metallic trace elements were determined by water extraction, according to the norm NF EN 13346. The measurement of Cu, Ni, Fe, Mo, Mn, Co and Zn concentrations was performed by plasma emission spectrometry, according to the NF EN ISO 11885. The concentrations of total P, K, Mg, Ca and Na were measured according to NF EN ISO 11885. Table 4 shows the main characteristics of the analyzed FWs from the different suppliers and the mixture used for feeding the reactors.

The results are in agreement with those commonly presented in the literature (Capson-Tojo et al., 2016). The TS content ranged from 10.1 to 40.0 % and the VS from 85.8 to 94.4 % VS/TS. Carbohydrates were the main component in all the samples (396-776 g·kg TS<sup>-1</sup>), followed by proteins (125-262 g·kg TS<sup>-1</sup>) and lipids (24.0-293 g·kg TS<sup>-1</sup>). Interestingly, the sample from fruit and vegetable distribution (mainly composed of vegetables such as leeks) had the highest concentration of proteins (262 g·kg TS<sup>-1</sup>), suggesting that some vegetables (*e.g.* leeks) might also contribute greatly to the high nitrogen content of FW (and thus to high TAN concentrations in the AD reactors). The high proportions of proteins led to high TKN concentrations and low C/N ratios (16.1 for the mixture), with values also in accordance with the literature (Capson-Tojo et al., 2016). High BMP values, ranging from 371 to 515 ml CH<sub>4</sub>·g VS<sup>-1</sup> were obtained, suggesting the suitability of this substrate for AD and a high potential energy recovery. As the theoretical methane yields are higher for lipids than for proteins or carbohydrates, higher BMPs were obtained in the samples with high lipid contents and low concentrations of carbohydrates (*i.e.* restaurants). Relatively high concentrations of macroelements (*i.e.* P, Ca, Mg, K or Na) were found but, as the levels were much lower than the reported inhibitory limits (Angelidaki and Ahring, 1992; Appels et al., 2008; Batstone et

al., 2000), no inhibition was expected. Interestingly, the concentration of TEs varied widely according to the FW source and typology. In FW mainly composed of vegetables and fruits much higher concentrations of TEs required for AD (such as Cu, Fe, Mn, Mo or Ni) were found when compared to the samples from meat-serving restaurant. This suggests that higher contents of FW mainly composed of fruits and vegetables may increase the TEs concentrations, helping to stabilize the AD process. As expected, Fe showed the highest concentrations, with values up to  $3 \text{ g}\cdot\text{l}^{-1}$  in FW from vegetable waste (fruit and vegetable distribution). Finally, the relatively high concentrations of VFAs (up to  $7.58 \text{ g COD}\cdot\text{kg}^{-1}$ ) and TAN (up to  $1.08 \text{ g}\cdot\text{kg TS}^{-1}$ ) suggest that the biodegradation of the substrates had already started during the storage period (inherent to the collection process and less than one week), proving also the high biodegradability and fast degradation kinetics of FW.

#### 2.4.2. Gas quantification and analysis

The amount of biogas produced in the pilot reactors was continually measured using Ritter MilliGascounters MGC-1 V3.0. The composition of the biogas (and the volume of gas produced in the batch essay presented in 2.3.) was determined as described in Cazier et al. (2015). For comparing the kinetics of methane production in the reactors, the experimental data corresponding to the methane yields were fit to the Gompertz equation (Zwietering et al., 1990) to estimate the kinetic parameters of the process. The least squares method was applied and the predicted values were plotted against the real data to evaluate the goodness of fit of the model. The resulting  $R^2$  and the p-value obtained from a Fisher's exact test were used as indicators.

#### 2.4.3. Analysis of metabolites and final products of the digestion

The concentrations of VFAs (*i.e.* acetic, propionic, butyric or valeric acids) and ionic species in the digestates were measured according to Motte et al. (2013). The concentration of FAN was calculated as a function of temperature, pH and TAN concentration (J. L. Chen et al.,

2014).

### 2.5. Thermodynamic calculations

To support the experimental findings, theoretical thermodynamic calculations were carried out. For this purpose, Equation 1 was used:

$$\Delta G' = \Delta G^0 + R \cdot T \cdot \ln \left( \frac{[C]^c \cdot [D]^d}{[A]^a \cdot [B]^b} \right) \quad \text{Equation 1}$$

Where  $\Delta G'$  is the variation of Gibbs free energy ( $\text{J} \cdot \text{mol}^{-1}$ ),  $\Delta G^0$  is the standard Gibbs free energy of the reaction ( $\text{J} \cdot \text{mol}^{-1}$ ),  $R$  is the ideal gas constant ( $8.314 \text{ J} \cdot \text{mol}^{-1} \cdot \text{K}^{-1}$ ),  $T$  is the temperature (K) and  $[I]^i$  are the concentrations and the stoichiometric coefficients in the reaction  $aA + bB \leftrightarrow cC + dD$ . When the line of zero  $\Delta G'$  for a reaction was calculated, the following conditions were assumed: 298 K, pH 7, 1 mM organic acids and 0.1 M  $\text{HCO}_3^-$ . These values were taken from Batstone et al. (2002) and the  $\Delta G^0$  from Zeeman (2005).

## 3. Results and discussion

### 3.1. Performance of the stabilization strategies in consecutive batch pilot reactors

The methane yields as well as the TS contents and the concentrations of HPr and TAN resulting from the different strategies evaluated for AD stabilization (working temperature of 30 °C (T30), co-digestion with PW (Co-PW), and TEs supplementation (Sup-TEs)) are shown in Figure 1.

#### 3.1.1. Methane production and gradual propionate accumulation

During the first 2 cycles (with a load of  $0.087 \text{ kg FW} \cdot \text{kg inoculum}^{-1}$ ), the reactors were clearly performant, with high methane yields achieved ( $\sim 500 \text{ ml CH}_4 \cdot \text{g VS}^{-1}$ ). However, differences were already observed between the conditions tested. The reactor T30 showed

much slower kinetics than that of the Control reactor (*i.e.* 35 days *vs.* 22 days to reach 500 ml CH<sub>4</sub>·g VS<sup>-1</sup>, respectively). This occurred simply because the lower reaction temperature slowed down the AD kinetics. This hypothesis was verified by adjusting the experimental results to the Gompertz equation. Taking the second feeding as example, the values of the maximum methane production rate and the lag phase were 48.1 ml CH<sub>4</sub>·g VS<sup>-1</sup>·d<sup>-1</sup> and 6.09 days for the Control reactor (R<sup>2</sup> 0.9964 and p-value of 1.71·10<sup>-23</sup>) and 29.7 ml CH<sub>4</sub>·g VS<sup>-1</sup>·d<sup>-1</sup> and 9.41 days for the reactor T30 (R<sup>2</sup> 0.994 and p-value of 1.03·10<sup>-41</sup>). Lower maximum methane production rates and longer lag phases confirmed the slower AD kinetics at 30 °C. In addition, the Co-PW reactor showed lower methane yields at similar digestion times. The maximum methane yields given by the Gompertz equation showed values of 368 ml CH<sub>4</sub>·g VS<sup>-1</sup> in the second cycle for the Co-PW reactor (R<sup>2</sup> 0.997 and p-value of 4.04·10<sup>-24</sup>), while a value of 564 ml CH<sub>4</sub>·g VS<sup>-1</sup> was obtained for the Control reactor. This happened because PW is a more recalcitrant substrate than FW, with a lower BMP (Capson-Tojo et al., 2017). Therefore, the global methane yields (expressed by total VS of substrate added) decreased. Moreover, it is interesting to mention that in the Co-PW reactor a concentration of HPr of about 4 g·l<sup>-1</sup> was reached already after the 1<sup>st</sup> feeding (Cycle 2).

As the performance was satisfactory, the organic load was doubled (0.173 kg FW·kg inoculum<sup>-1</sup>) in all the reactors in the 3<sup>rd</sup> and 4<sup>th</sup> cycles. In addition, the reactor Sup-TEs was started. Again, satisfactory methane yields were achieved (~500 ml CH<sub>4</sub>·g VS<sup>-1</sup>), which led to high volumetric productivities (up to 16 l CH<sub>4</sub>·l<sup>-1</sup>). However, at the end of the 3<sup>rd</sup> cycle, significant amounts of HPr were detected in all conditions, with concentrations up to 17.0 g·l<sup>-1</sup> in the Co-PW reactor. This HPr accumulation jeopardized the methane production kinetics and increased the lag phases in the methane production. Taking the results from the Gompertz equation of the Control reactor as example, while in the third feeding (negligible initial HPr concentrations) the maximum methane production rate and the lag phase were 40.4 ml CH<sub>4</sub>·g

$\text{VS}^{-1} \cdot \text{d}^{-1}$  and 3.62 days ( $R^2$  0.996 and p-value of  $3.82 \cdot 10^{-21}$ ), these values were  $30.5 \text{ ml CH}_4 \cdot \text{g VS}^{-1} \cdot \text{d}^{-1}$  and 6.40 days ( $R^2$  0.997 and p-value of  $2.42 \cdot 10^{-41}$ ) for the same reactor in the fifth cycle (with initial HPr concentrations of  $3.3 \text{ g} \cdot \text{l}^{-1}$ ), indicating slower AD kinetics.

Nevertheless, a clear improvement in the kinetics of methane production and in the reduction of HPr accumulation was observed in Sup-TEs when compared with the other conditions (*i.e.* methane yields of  $462 \text{ ml CH}_4 \cdot \text{g VS}^{-1}$  achieved in 14 days *vs.* 20 days for the Control reactor in the 3<sup>rd</sup> cycle), suggesting a positive effect of the TEs supplementation. By comparing the kinetic parameters of the Sup-TEs reactor with the Control reactor right after its start-up (3<sup>rd</sup> cycle), the Gompertz equation served to verify this hypothesis. While the maximum methane production rate and the lag phase in the Sup-TEs reactor were  $44.7 \text{ ml CH}_4 \cdot \text{g VS}^{-1} \cdot \text{d}^{-1}$  and 2.00 days ( $R^2$  0.978 and p-value of  $8.31 \cdot 10^{-15}$ ), these values were  $40.4 \text{ ml CH}_4 \cdot \text{g VS}^{-1} \cdot \text{d}^{-1}$  and 3.62 days ( $R^2$  0.996 and p-value of  $3.82 \cdot 10^{-21}$ ) in the Control reactor. Thus, in the 5<sup>th</sup> feeding cycle, the load was increased in the Sup-TEs reactor to  $0.255 \text{ kg FW} \cdot \text{kg inoculum}^{-1}$ . Although methane was produced efficiently, this load increase led to a slightly lower methane yield and to a sharp increase in the HPr concentration, up to  $3.4 \text{ g} \cdot \text{l}^{-1}$ . A second feeding with the same load (6<sup>th</sup> cycle) caused acidification of the reactor, with pH values down to 5.9 and HPr and HAc concentrations of  $7.30 \text{ g} \cdot \text{l}^{-1}$  and  $16.1 \text{ g} \cdot \text{l}^{-1}$ , respectively (see Table 5, showing the concentrations of both acids after each cycle). This suggested that a load of  $0.255 \text{ kg FW} \cdot \text{kg inoculum}^{-1}$  was too high for the system. To verify if this load would lead to inhibition in all the conditions, an additional experiment (not presented) was carried out. Digestates from the four reactors were used as inoculum for lab-scale batch reactors at a load of  $0.255 \text{ kg FW} \cdot \text{kg inoculum}^{-1}$  (that leading to inhibition in the Sup-TEs pilot). All the batch reactors were acidified (data not shown), confirming the results from the pilot reactors.

Therefore, the Sup-TEs reactor was restarted in day 133 with digestate from the Control reactor and the load was reduced to  $0.173 \text{ kg FW} \cdot \text{kg inoculum}^{-1}$  (the maximum applied in the

other three reactors). However, even at this load HPr continued to accumulate in the reactors, slowing down the methane kinetics (longer lag phases) and endangering the AD process. With much lower maximum methane production rates and longer lag phases than previously, the values of the kinetics parameters in the 6<sup>th</sup> feeding of the Control reactor serve to illustrate this decrease of the AD kinetics: 23.9 ml CH<sub>4</sub>·g VS<sup>-1</sup>·d<sup>-1</sup> and 13.3 days (R<sup>2</sup> 0.998 and p-value of 1.76·10<sup>-36</sup>), respectively. The co-digestion reactor (Co-PW) showed the most important build-up of HPr, with concentrations up to 21.6 g·l<sup>-1</sup> detected after the 4<sup>th</sup> cycle and pH values down to 6.5. Interestingly, the substrate conversion (estimated as the sum of methane and VFAs) remained relatively constant. At this point, the feeding of this reactor was stopped to evaluate if the concentration of HPr would decrease without addition of an external substrate. After two months, no significant decrease was observed.

Concerning the TS contents, average values from 6.5±0.6 to 7.9±0.6 % were observed in the reactors Control, T30 and Sup-TEs. Due to the addition of PW, the Co-PW reactor reached higher TS values, of 11.3±0.3 % after the 3<sup>rd</sup> Cycle. The high TS contents in Co-PW were caused by the high TS proportion of the PW and its lower degradability when compared with FW.

### *3.1.2. Role of the concentrations of FAN and metabolites in propionate accumulation*

The FAN concentrations were also affected by the working conditions. Since no specific strategies were applied to reduce the FAN concentrations, the Control and Sup-TEs reactors showed the highest concentrations (1077 and 780 mg FAN·l<sup>-1</sup>, respectively). Applying a temperature of 30 °C in T30 allowed reducing this value to 691 mg FAN·l<sup>-1</sup> by displacement of the NH<sub>4</sub><sup>+</sup>-NH<sub>3</sub> equilibrium towards NH<sub>4</sub><sup>+</sup>. In addition, the co-digestion reactor (Co-PW) showed also lower TAN levels (520 mg FAN·l<sup>-1</sup>) because of the high C/N ratio of PW, which diluted the TAN concentrations (up to 7.1 g·l<sup>-1</sup> in Co-PW vs. 9.5 g·l<sup>-1</sup> in the Control reactor). It must be mentioned that the much lower concentrations of FAN in Co-PW were also related

to the lower pH values in this reactor due to the higher HPr concentrations. While in the other reactors the pH ranged between 7.89 and 8.16, the pH in Co-PW ranged between 7.85 and 6.49. This affected greatly the  $\text{NH}_4^+ \text{-NH}_3$  equilibrium, favoring the formation of  $\text{NH}_4^+$ .

In order to understand why HPr accumulated in the reactors, it was required to pay attention to the high TAN/FAN concentrations and its consequences, as well as to the concentrations of AD metabolites. With this purpose Figures 2 and 3 are shown. Figure 2 represents the different pathways and reactions involved in methane production during AD and Figure 3 plots the theoretical lines of zero  $\Delta G'$  for the same reactions at different acetate concentrations and hydrogen partial pressures. As aforementioned, acetoclastic archaea are inhibited over  $2.8\text{-}3.0 \text{ g TAN}\cdot\text{l}^{-1}$  (De Vrieze et al., 2012) and therefore the acetoclastic pathway (acetoclastic methanogenesis-AM; dashed lines in Figure 2) becomes less important than in non-stressed AD conditions. As a consequence, syntrophic acetate oxidation (SAO) and hydrogenotrophic methanogenesis (HM; continuous lines in Figure 2) becomes the predominant methane producing pathway (De Vrieze et al., 2012; Jiang et al., 2017). Thus, mediated interspecies electron transfer (MIET), using hydrogen or formate as electron shuttles, becomes a critical step of the global process. These syntrophic interactions are particularly important for syntrophic propionate oxidation (SPO; reaction (i) in Figure 2). HPr can only be degraded by coupling SPO and SAO with HM. In addition, as acetic acid (HAc) and hydrogen/formate are products of HPr degradation (reaction (i) in Figure 2), SPO becomes thermodynamically unfavorable by product-induced feedback inhibition if these compounds accumulate in the reactor (which is more likely to occur during HM). It must be mentioned that, as the thermodynamics and stoichiometry of hydrogen and formate are virtually identical, only one has been considered in Figures 2 and 3 (Batstone et al., 2002). As it can be observed in Figure 3, while acetoclastic methanogenesis (AM) is thermodynamically favorable in almost the whole range presented (therefore being

predominant in non-stressed AD), there is only a small thermodynamic window in which SAO, SPO and HM can occur simultaneously (yellowish region in Figure 3). Figure 3 offers a possible explanation for the HPr accumulation observed. During batch AD of FW, an initial accumulation of VFAs (mainly HAc) occurs at the beginning of the process (Wanli Zhang et al., 2015a). In the present study, transient HAc concentrations of  $17.2 \text{ g}\cdot\text{l}^{-1}$  (0.29 M) were detected during the first days after reactor loading. In addition, before re-loading the pilots, the minimal concentrations of HAc were higher than  $2\cdot 10^{-3} \text{ M}$  (Table 5). This means that throughout the operational period in all the reactors the concentrations of HAc were mostly within a range where the degradation of HAc was more thermodynamically feasible than that of HPr (region at the right of the vertical red line in Figure 3). This jeopardized the growth of syntrophic propionate oxidizers, which are slow-growing microorganisms (de Bok et al., 2004), causing eventually accumulation of HPr. Thus, it can be hypothesized that SPO was not thermodynamically favorable due to the high concentrations of HAc and hydrogen/formate in the reactors.

### *3.1.3. Role of the operating mode in propionate accumulation*

The first point to mention in this section is that a main drawback of batch operation when compared with continuous mode is the initial substrate overload that occurs after feeding, which can lead to high transient VFA concentrations. In continuous operation, this overloading does not exist and therefore the concentrations of HAc or hydrogen are never as high as in batch operation. As shown in Figure 3, if lower concentrations of HAc or hydrogen are present, SPO is favored. In other words, at equivalent loads in continuous reactors, the initial overload of substrate occurring in batch experiments is avoided and therefore the initial accumulation of intermediate compounds is less important, thus reducing the initial accumulation of HPr. Continuous operation in continuous-stirred tank reactors (CSTRs) may be a more appropriate option when compared to batch reactors (even if it is more complex

technically).

The observed accumulation of HPr during FW AD has been commonly reported in the literature in continuous or single batch reactors. For example, in an AD plant of 900 m<sup>3</sup> digesting FW, Banks et al. (2011) observed HPr concentrations up to 14 g·l<sup>-1</sup> after 426 days of operation at an average OLR of 2.5 g VS·l<sup>-1</sup>·d<sup>-1</sup>. These results were confirmed by different semi-continuous lab-scale studies, in which HPr build-up during FW AD at low OLRs, directly inhibiting the AD process or jeopardizing its performance (Zhang et al., 2013; Wanli Zhang et al., 2015a, 2015b). However, these studies showed that the addition of TEs or co-substrates rich in those elements (such as piggery wastewater or fresh leachate from the storage of a municipal solid waste incineration plant) avoided the HPr accumulation and stabilized the AD process, even at high OLRs (6-8 g VS·l<sup>-1</sup>·d<sup>-1</sup>). A possible reason behind the accumulation of HPr in the present study even when TEs were supplied may be the initial substrate overload that exists after feeding during sequential batch operation.

In addition, the strategy used for feeding the successive batch reactors may also have led to a key issue. In the present experiment, the loading strategy consisted on starting a new batch by monitoring only the methane kinetics (*i.e.* the reactors were fed once a biogas plateau or a determined methane yield was achieved) and no attention was paid to the VFA concentrations. Therefore, the reactors were reloaded when the concentrations of HAc were approaching values low enough to allow HPr oxidation (right region of Figure 3), increasing again the HAc concentrations and avoiding the development of syntrophic propionic degraders (slow-growing bacteria). Thus, the batch time was never long enough to allow HPr degradation. This also implies that if the process is to be scaled-up, the biogas production should not be the sole parameter to evaluate if the re-loading is feasible. The VFA concentrations must also be monitored. It must be mentioned that this issue would not have been observed after only one batch operation.

Co-digesting FW with a substrate having a higher C/N ratio (*i.e.* PW) did not avoid HPr accumulation. In fact, at the co-digestion proportions applied (75 % FW:25 % PW w/w), the dilution of TAN (up to  $7.0 \text{ g}\cdot\text{l}^{-1}$  in the reactor) was not enough to avoid inhibition of acetoclastic methanogens. On the contrary, the co-digestion reactor showed the worst methane production performance and the highest HPr concentrations (up to  $21.6 \text{ g}\cdot\text{l}^{-1}$ ). As PW is degraded more slowly than FW, a hypothesis explaining this observation could be that the release of VFAs during AD was also slower, causing relatively higher HAc concentrations in the reactor for a longer period of time. Consequently, according to Figure 3, SPO was not feasible. Another possible explanation is that PW addition simply favored the synthesis of HPr. More significant HPr accumulation during co-digestion of card packaging and FW when compared to FW mono-digestion were also reported by Zhang et al. (2012) in continuous reactors. More research must be carried out to elucidate the reasons behind this observation.

### *3.2. Favoring consumption of propionic acid after its accumulation*

In order to screen different possibilities to avoid HPr accumulation or to favor its consumption, the experimental design presented in Table 3 was carried out. As described above, the influence of the addition of TEs and GAC on the VFA consumption was tested using digestate from the Co-PW reactor (with concentrations of HAc and HPr of  $6.41$  and  $21.0 \text{ g}\cdot\text{l}^{-1}$  respectively). Two different TEs concentrations (equivalent to  $100$  and  $500 \text{ mg Fe}\cdot\text{l}^{-1}$ ) and one of GAC ( $10 \text{ g}\cdot\text{l}^{-1}$ ) were tested. The effect of diluting the digestate (doubling its volume adding water) was also assessed. The dynamics of methane production and concentrations of HAc and HPr are presented in Figure 4.

According to the results presented in Figure 4, three successive phases can be identified. During the first phase, corresponding to about the first 28 days (vertical red line in Figure 4), methane production occurred because of the degradation of HAc and readily available residual substrates but HPr was not consumed in any condition. At this end of this phase, the

HAc concentration was approximately of  $0.4 \text{ g}\cdot\text{l}^{-1}$  ( $7\cdot 10^{-3} \text{ M}$ ) in all conditions, meaning that SPO should have been thermodynamically feasible if the partial pressure of hydrogen (or the equivalent concentration of formate) is low enough (Figure 3). However, in the case of undiluted reactors, a “stable phase” occurred during which the concentrations of HPr and HAc did not vary and no significant production of methane was observed (period between both vertical lines in Figure 4). After about 52 days, HPr started to be degraded in those conditions (vertical blue line in Figure 4). Simultaneously, a slight increase in the HAc concentrations was observed since HPr was degraded into HAc (resulting in an increase of the HAc concentrations up to  $5.3 \text{ g}\cdot\text{l}^{-1}$ ; in agreement with Equation (i) in Figure 3) and methane was also produced (probably by SAO and HM). Interestingly, in the case of the diluted reactor (1/2Dilution), SPO started earlier, right after the first phase. This can be explained by the lower concentration of electron shuttles (hydrogen and/or formate) due to the addition of water. In this experiment, the total consumption of HPr took between 66 and 114 days, confirming that the degradation of this VFA is clearly a problem after its build-up. Even if the global behavior of the undiluted reactors (Control, addition of TES, addition of GAC) was similar, slight differences can be highlighted. The addition of TEs (5xTEs) improved slightly the kinetics of HPr degradation when compared to the Control reactor, probably by favoring the synthesis of formate dehydrogenase (Banks et al., 2012). Interestingly, SPO was clearly improved when adding GAC. The results indicate that the most plausible explanation is the occurrence of DIET in the reactors. As shown in Figure 4B, HAc was degraded faster when GAC was supplemented into the reactors, which favored slightly also the methane production. HAc can be degraded through DIET via direct interaction between an electroactive bacteria and hydrogenotrophic methanogens (Lee et al., 2016), which may explain the better performance in this condition. This led, not only to lower HAc concentrations in the reactors, but also to lower concentrations of electron shuttles, whose

formation was avoided (the electrons were directly exchanged). As the concentrations of both HAc and hydrogen/formate were lower, SPO became thermodynamically favorable earlier (Figure 3). Moreover, also SPO may have occurred directly through DIET (Zhao et al., 2016). Other than DIET, the steeper slope of HPr degradation in the GAC reactor also suggests that the growth of HPr oxidizing bacteria during the exponential phase was promoted, probably through biofilm formation onto the GAC surface, allowing syntrophic interactions to occur. Further research must be carried out to elucidate if the process performance can be improved by allowing the growth of HPr oxidizers, achieving eventually a stable HPr-degrading community (with and without the addition of support materials such as GAC). In addition, dilution of the substrate can be an option to solve HPr accumulation. Although this alternative is widely applied in industrial AD of solid waste for substrate pretreatment before AD, it leads to greater reactor volumes, lower energy balances and higher amounts of digestate to be dealt with and therefore is a practice to be avoided in the future. Promising options such as GAC addition and TEs optimization (and its combination) have the potential of improving greatly the performance of FW AD (*i.e.* improving the biogas productivities and reducing the retention times) and deserve further research.

#### 4. Conclusions

Methane was efficiently produced in successive batch reactors ( $\sim 500 \text{ mlCH}_4 \cdot \text{gVS}^{-1}$ ;  $16 \text{ lCH}_4 \cdot \text{l}^{-1}$ ) but HPr accumulated in all of them, with concentrations up to  $21.6 \text{ g} \cdot \text{l}^{-1}$ . This led to acidification at high substrate loads. Co-digestion with PW led to the highest HPr concentration. Supplementation of trace elements stabilized AD, improving the kinetics and allowing greater substrate loads. However, it could not avoid HPr accumulation. Batch experiments suggested that GAC addition, TEs supplementation and dilution can favor HPr consumption. Further research must be carried out to elucidate the effect of these promising

options to prevent acid accumulation and/or favor its consumption.

### Acknowledgement

The authors gratefully acknowledge Suez for financing this research under the CIFRE convention N° 2014/1146. In addition, they want to express their gratitude to the Communauté d'Agglomération du Grand Narbonne (CAGN) for the financial support.

### References

1. Angelidaki, I., Ahring, B.K., 1992. Effects of free long-chain fatty acids on thermophilic anaerobic digestion. *Appl. Microbiol. Biotechnol.* 37, 808–812.
2. APHA, 2005. *Standard Methods for the Examination of Water and Wastewater*. American Public Health Association, Washington, DC.
3. Appels, L., Baeyens, J., Degève, J., Dewil, R., 2008. Principles and potential of the anaerobic digestion of waste-activated sludge. *Prog. Energy Combust. Sci.* 34, 755–781.
4. Asato, C.M., Gonzalez-Estrella, J., Jerke, A.C., Bang, S.S., Stone, J.J., Gilcrease, P.C., 2016. Batch anaerobic digestion of synthetic military base food waste and cardboard mixtures. *Bioresour. Technol.* 216, 894–903.
5. Banks, C.J., Chesshire, M., Heaven, S., Arnold, R., 2011. Anaerobic digestion of source-segregated domestic food waste: Performance assessment by mass and energy balance. *Bioresour. Technol.* 102, 612–620.
6. Banks, C.J., Chesshire, M., Stringfellow, A., 2008. A pilot-scale trial comparing mesophilic and thermophilic digestion for the stabilisation of source segregated kitchen waste. *Water Sci. Technol.* 58, 1475–1481.
7. Banks, C.J., Zhang, Y., Jiang, Y., Heaven, S., 2012. Trace element requirements for stable food waste digestion at elevated ammonia concentrations. *Bioresour. Technol.* 104, 127–135.
8. Batstone, D.J., Keller, J., Angelidaki, I., Kalyuzhny, S. V, Pavlostathis, S.G., Rozzi, A., Sanders, W.T.M., Siegrist, H., Vavilin, V.A., 2002. *Anaerobic digestion model no. 1 (ADM1)*. IWA Publishing.
9. Batstone, D.J., Keller, J., Newell, R.B., Newland, M., 2000. Modelling anaerobic degradation of complex wastewater. I: model development. *Bioresour. Technol.* 75, 67–74.
10. Bernstad, A., Wenzel, H., la Cour Jansen, J., 2016. Identification of decisive factors for greenhouse gas emissions in comparative lifecycle assessments of food waste management – An analytical review. *J. Clean Prod.* 119, 13–24.
11. Capson-Tojo, G., Rouez, M., Crest, M., Steyer, J.-P., Delgenès, J.-P., Escudíé, R.,

2016. Food waste valorization via anaerobic processes: a review. *Rev. Env. Sci. Biotechnol.* 15, 499–547.
12. Capson-Tojo, G., Trably, E., Rouez, M., Crest, M., Steyer, J.-P., Delgenès, J.-P., Escudie, R., 2017. Dry anaerobic digestion of food waste and cardboard at different substrate loads, solid contents and co-digestion proportions. *Bioresour. Technol.* 233, 166–175.
  13. Cazier, E.A., Trably, E., Steyer, J.P., Escudie, R., 2015. Biomass hydrolysis inhibition at high hydrogen partial pressure in solid-state anaerobic digestion. *Bioresour. Technol.* 190, 106–113.
  14. Chen, J.L., Ortiz, R., Steele, T.W.J., Stuckey, D.C., 2014. Toxicants inhibiting anaerobic digestion: a review. *Biotechnol. Adv.* 32, 1523–34.
  15. Chen, X., Yan, W., Sheng, K., Sanati, M., 2014. Comparison of high-solids to liquid anaerobic co-digestion of food waste and green waste. *Bioresour. Technol.* 154, 215–221.
  16. Cogan, M., Antizar-Ladislao, B., 2016. The ability of macroalgae to stabilise and optimise the anaerobic digestion of household food waste. *Biomass Bioenergy* 86, 146–155.
  17. Dang, Y., Holmes, D.E., Zhao, Z., Woodard, T.L., Zhang, Y., Sun, D., Wang, L.-Y., Nevin, K.P., Lovley, D.R., 2016. Enhancing anaerobic digestion of complex organic waste with carbon-based conductive materials. *Bioresour. Technol.* 220, 516–522.
  18. de Bok, F.A.M., Plugge, C.M., Stams, A.J.M., 2004. Interspecies electron transfer in methanogenic propionate degrading consortia. *Water Res.* 38, 1368–1375.
  19. De Vrieze, J., Hennebel, T., Boon, N., Verstraete, W., 2012. Methanosarcina: The rediscovered methanogen for heavy duty biomethanation. *Bioresour. Technol.* 112, 1–9.
  20. Dubois, M., Gilles, K.A., Hamilton, J.K., Rebers, P.A., Smith, F., 1956. Colorimetric Method for Determination of Sugars and Related Substances. *Anal. Chem.* 28, 350–356.
  21. Dung Thi, N.B., Lin, C.-Y., Kumar, G., 2016. Electricity generation comparison of food waste-based bioenergy with wind and solar powers: a mini review. *Sust. Env. Res.* 26 (5), 197-202.
  22. Ebner, J.H., Labatut, R.A., Lodge, J.S., Williamson, A.A., Trabold, T.A., 2016. Anaerobic co-digestion of commercial food waste and dairy manure: Characterizing biochemical parameters and synergistic effects. *Waste Manag.* 52, 286–294.
  23. Fagbohunge, M.O., Herbert, B.M.J., Hurst, L., Ibeto, C.N., Li, H., Usmani, S.Q., Semple, K.T., 2017. The challenges of anaerobic digestion and the role of biochar in optimizing anaerobic digestion. *Waste Manag.* 61, 236–249.
  24. Ganesh, R., Torrijos, M., Sousbie, P., Steyer, J.P., Lugardon, A., Delgenes, J.P., 2013. Anaerobic co-digestion of solid waste: Effect of increasing organic loading rates and characterization of the solubilised organic matter. *Bioresour. Technol.* 130, 559–69.
  25. Jiang, Y., Banks, C., Zhang, Y., Heaven, S., Longhurst, P., 2017. Quantifying the percentage of methane formation via acetoclastic and syntrophic acetate oxidation pathways in anaerobic digesters. *Waste Manag.* In Press.

26. Jimenez, J., Vedrenne, F., Denis, C., Mottet, A., Déléris, S., Steyer, J.-P., Rivero, J.A.C., 2013. A statistical comparison of protein and carbohydrate characterisation methodology applied on sewage sludge samples. *Water Res.* 47, 1751–1762.
27. Kim, D.-H., Oh, S.-E., 2011. Continuous high-solids anaerobic co-digestion of organic solid wastes under mesophilic conditions. *Waste Manag.* 31, 1943–1948.
28. Kim, M., Chowdhury, M.M.I., Nakhla, G., Keleman, M., 2017. Synergism of co-digestion of food wastes with municipal wastewater treatment biosolids. *Waste Manag.* 61, 473-483.
29. Lee, J.Y., Lee, S.H., Park, H.D., 2016. Enrichment of specific electro-active microorganisms and enhancement of methane production by adding granular activated carbon in anaerobic reactors. *Bioresour. Technol.* 205, 205–212.
30. Motte, J.-C., Escudié, R., Beaufile, N., Steyer, J.-P., Bernet, N., Delgenès, J.-P., Dumas, C., 2014. Morphological structures of wheat straw strongly impacts its anaerobic digestion. *Ind. Crops Prod.* 52, 695–701.
31. Motte, J.-C., Trably, E., Escudié, R., Hamelin, J., Steyer, J.-P., Bernet, N., Delgenès, J.-P., Dumas, C., 2013. Total solids content: a key parameter of metabolic pathways in dry anaerobic digestion. *Biotechnol. Biofuels* 6, 164.
32. Motte, J.-C., Watteau, F., Escudié, R., Steyer, J.-P., Bernet, N., Delgenès, J.-P., Dumas, C., 2015. Dynamic observation of the biodegradation of lignocellulosic tissue under solid-state anaerobic conditions. *Bioresour. Technol.* 191, 322–326.
33. Qiang, H., Lang, D.-L., Li, Y.-Y., 2012. High-solid mesophilic methane fermentation of food waste with an emphasis on Iron, Cobalt, and Nickel requirements. *Bioresour. Technol.* 103, 21–7.
34. Qiang, H., Niu, Q., Chi, Y., Li, Y., 2013. Trace metals requirements for continuous thermophilic methane fermentation of high-solid food waste. *Chem. Eng. J.* 222, 330–336.
35. Rajagopal, R., Massé, D.I., Singh, G., 2013. A critical review on inhibition of anaerobic digestion process by excess ammonia. *Bioresour. Technol.* 143, 632–641.
36. Stoknes, K., Scholwin, F., Krzesiński, W., Wojciechowska, E., Jasińska, A., 2016. Efficiency of a novel “Food to waste to food” system including anaerobic digestion of food waste and cultivation of vegetables on digestate in a bubble-insulated greenhouse. *Waste Manag.* 56, 466–476.
37. Yirong, C., Heaven, S., Banks, C.J., 2015. Effect of a Trace Element Addition Strategy on Volatile Fatty Acid Accumulation in Thermophilic Anaerobic Digestion of Food Waste. *Waste Biomass Valorization* 6, 1–12.
38. Zeeman, G., 2005. *Anaerobic Wastewater Treatment*, 2005th ed. Wageningen University, Wageningen.
39. Zhang, C., Xiao, G., Peng, L., Su, H., Tan, T., 2013. The anaerobic co-digestion of food waste and cattle manure. *Bioresour. Technol.* 129, 170–176.
40. Zhang, L., Jahng, D., 2012. Long-term anaerobic digestion of food waste stabilized by trace elements. *Waste Manag.* 32, 1509–1515.
41. Zhang, L., Lee, Y.-W., Jahng, D., 2011. Anaerobic co-digestion of food waste and piggery wastewater: Focusing on the role of trace elements. *Bioresour. Technol.* 102,

- 5048–5059.
42. Zhang, W., Wu, S., Guo, J., Zhou, J., Dong, R., 2015. Performance and kinetic evaluation of semi-continuously fed anaerobic digesters treating food waste: role of trace elements. *Bioresour. Technol.* 178, 297–305.
  43. Zhang, W., Zhang, L., Li, A., 2015a. Enhanced anaerobic digestion of food waste by trace metal elements supplementation and reduced metals dosage by green chelating agent [S, S]-EDDS via improving metals bioavailability. *Water Res.* 84, 266–77.
  44. Zhang, W., Zhang, L., Li, A., 2015b. Anaerobic co-digestion of food waste with MSW incineration plant fresh leachate: process performance and synergistic effects. *Chem. Eng. J.* 259, 795–805.
  45. Zhang, Y., Banks, C.J., Heaven, S., 2012. Co-digestion of source segregated domestic food waste to improve process stability. *Bioresour. Technol.* 114, 168–178.
  46. Zhao, Z., Zhang, Y., Yu, Q., Dang, Y., Li, Y., Quan, X., 2016. Communities stimulated with ethanol to perform direct interspecies electron transfer for syntrophic metabolism of propionate and butyrate. *Water Res.* 102, 475–484.
  47. Zwietering, M.H., Jongenburger, I., Rombouts, F.M., Van't Riet, K., 1990. Modeling of the bacterial growth curve. *Applied and environmental microbiology* 56, 1875–1881.

### Figure and table captions

**Figure 1.** Kinetics of methane production in the pilot reactors. The concentrations of propionic acid and TAN after each feeding cycle are also presented. The acetic acid concentrations are shown in Table 5. The numbers on the top of the methane curves stand for the loads applied for each batch ( $\text{kg FW} \cdot \text{kg inoculum}^{-1}$ ). The grey-shaded methane curves correspond to conditions equivalent to those in the Control reactor (1) and to the results of the Control reactor (2)

**Figure 2.** Different pathways involved in methane production during AD. The dashed lines represent the pathway inhibited at the high TAN/FAN concentrations associated with FW AD. The main reactions hypothesized to occur during FW AD are shown

**Figure 3.** Lines of zero  $\Delta G'$  for the reactions shown in Figure 2 at different acetate concentrations and hydrogen partial pressures. They were calculated assuming 298 K, pH 7, 1 mM HPr and 0.1 M  $\text{HCO}_3^-$ . The  $\Delta G^0$  were taken from Zeeman (2005). SPO, SAO, HM and AM stand for syntrophic propionate oxidation, syntrophic acetate oxidation, hydrogenotrophic methanogenesis and acetoclastic methanogenesis, respectively

**Figure 4.** Cumulative methane productions (A) and concentrations of acetic acid (B) and propionic acid (C) during the batch experiments. The reactors were incubated at 37 °C for a period of 142 days

**Table 1.** Working conditions in the pilot reactors

**Table 2.** Loading regime applied to the pilot reactors (kg FW·kg inoculum<sup>-1</sup>)

**Table 3.** Experimental design of the batch essay for favoring VFA consumption. The working temperature was 37 °C. The inoculum was taken from the Co-PW reactor

**Table 4.** Characteristics of the food waste samples

**Table 5.** Concentrations of acetic and propionic acids in the pilots after each feeding cycle

ACCEPTED MANUSCRIPT

**Table 1.** Working conditions in the pilot reactors

Reactor	Substrate	Initial working volume (l)	Working temperature (°C)
Control	FW <sup>1</sup>	20	37
T30	FW <sup>1</sup>	7.5	30
Co-PW	FW <sup>1</sup> + PW <sup>2</sup>	7.5 – 10	37
Sup-TEs	FW <sup>1</sup> + TEs <sup>3</sup>	8.4 – 10	37

1. Food waste
2. Paper waste
3. Trace elements

ACCEPTED MANUSCRIPT

**Table 2.** Loading regime applied to the pilot reactors (kg FW·kg inoculum<sup>-1</sup>)

Reactor\Cycle #	1	2	3	4	5	6	7
<b>Control</b>	0.087	0.087	0.173	0.173	0.173	0.173	na <sup>1</sup>
<b>T30</b>	0.087 <sup>2</sup>	0.087	0.173	0.173	na <sup>1</sup>	na <sup>1</sup>	na <sup>1</sup>
<b>Co-PW</b>	0.087 <sup>2</sup>	0.087	0.173	0.173	0.173	na <sup>1</sup>	na <sup>1</sup>
<b>Sup-TEs</b>	0.087 <sup>3</sup>	0.087 <sup>3</sup>	0.173	0.173	0.255	0.255	0.173

1. Not applicable

2. Conditions equivalent to the Control reactor

3. Results of the Control reactor

**Table 3.** Experimental design of the batch assay for favoring VFA consumption. The working temperature was 37 °C. The inoculum was taken from the Co-PW reactor

Reactor	Initial working volume (ml)	TEs concentration (mg Fe·l <sup>-1</sup> ) <sup>1</sup>	GAC concentration (g·l <sup>-1</sup> )
Control	288	-	-
TEs	291	100	-
5xTEs	303	500	-
GAC	291	-	10
1/2Dilution	577	-	-

<sup>1</sup> Concentrations expressed in mg Fe·l<sup>-1</sup> to facilitate comprehension. All the TEs mentioned in section 2.2 were also added

**Table 4.** Characteristics of the food waste samples

Parameter	Fast food restaurant	Restaurant	Supermarket	Fruit and vegetable supermarket	Fruit and vegetable distribution	Mixture
TS (%)	34.3	40.1	10.2	10.0	10.6	21.0
VS/TS (%)	93.1	88.5	94.4	89.8	85.8	90.3
Carbohydrates (g·kg TS <sup>-1</sup> )	396	524	762	776	634	618
Proteins (g·kg TS <sup>-1</sup> )	230	190	129	125	262	187
Lipids (g·kg TS <sup>-1</sup> )	293	127	62.6	24.0	99.0	121
BMPs (ml CH <sub>4</sub> ·g VS <sup>-1</sup> )	515	449	377	388	371	420
pH	5.20	5.40	4.70	4.70	5.10	5.02
TOC (g·kg TS <sup>-1</sup> )	454	431	457	452	439	447
TAN (g·kg TS <sup>-1</sup> )	0.69	1.08	0.53	0.40	1.80	0.90
TKN (g·kg TS <sup>-1</sup> )	36.7	30.4	20.7	19.9	42.0	30.0
C/N (TOC/TKN)	12.4	14.1	21.7	21.8	10.3	16.1
P <sub>2</sub> O <sub>5</sub> (g·kg TS <sup>-1</sup> )	7.59	27.0	5.76	6.97	14.2	12.3
CaO (g·kg TS <sup>-1</sup> )	14.0	42.4	6.70	12.9	10.0	17.2
MgO (g·kg TS <sup>-1</sup> )	1.21	1.86	2.56	2.49	5.16	2.66
K <sub>2</sub> O (g·kg TS <sup>-1</sup> )	9.33	13.7	31.4	32.8	43.9	26.2
Na (g·kg TS <sup>-1</sup> )	9.89	7.69	0.95	0.74	1.97	4.25
Co (mg·kg TS <sup>-1</sup> )	< 9.75	< 9.75	< 9.75	< 9.75	< 9.75	< 9.75
Cu (mg·kg TS <sup>-1</sup> )	4.92	9.43	12.14	11.68	18.03	11.2
Fe (mg·kg TS <sup>-1</sup> )	268	294	731	1227	3049	1114
Mn (mg·kg TS <sup>-1</sup> )	12.5	10.3	30.7	30.2	54.3	27.6
Mo (mg·kg TS <sup>-1</sup> )	< 0.35	0.47	0.48	0.85	4.49	1.26
Zn (mg·kg TS <sup>-1</sup> )	52.6	36.3	20.3	27.6	55.3	38.4
Ni (mg·kg TS <sup>-1</sup> )	< 1.99	< 1.99	< 1.99	2.06	3.87	1.19
Acetate (g·kg <sup>-1</sup> )	6.14	5.59	1.39	4.21	4.18	4.30
Propionate (g·kg <sup>-1</sup> )	0.01	< 5·10 <sup>-4</sup>	< 5·10 <sup>-4</sup>	< 5·10 <sup>-4</sup>	< 5·10 <sup>-4</sup>	< 5·10 <sup>-4</sup>
Total VFAs (g COD·kg <sup>-1</sup> )	7.58	6.72	1.61	4.76	4.73	5.08

**Table 5.** Concentrations of acetic and propionic acids in the pilots after each feeding cycle

Compound	Reactor	Cycle 1	Cycle 2	Cycle 3	Cycle 4	Cycle 5	Cycle 6	Cycle 7
Acetic Acid <sup>2</sup>	Control	0.138	0.247	0.214	0.434	1.052	0.270	na <sup>1</sup>
	T30	na <sup>1</sup>	0.117	0.147	0.238	na <sup>1</sup>	na <sup>1</sup>	na <sup>1</sup>
	Co-PW	na <sup>1</sup>	0.285	0.328	0.650	6.41	na <sup>1</sup>	na <sup>1</sup>
	Sup-TEs	na <sup>1</sup>	na <sup>1</sup>	0.106	0.856	1.39	16.1	0.204
Propionic Acid <sup>3</sup>	Control	0.004	0.174	1.91	3.33	5.88	7.65	na <sup>1</sup>
	T30	na <sup>1</sup>	0.004	3.64	5.11	na <sup>1</sup>	na <sup>1</sup>	na <sup>1</sup>
	Co-PW	na <sup>1</sup>	4.05	7.57	17.0	21.0	na <sup>1</sup>	na <sup>1</sup>
	Sup-TEs	na <sup>1</sup>	na <sup>1</sup>	0.00	1.32	3.40	7.30	7.135

1. Not applicable

2. Molecular weight of 60.05 g·mol<sup>-1</sup>

3. Molecular weight of 74.08 g·mol<sup>-1</sup>

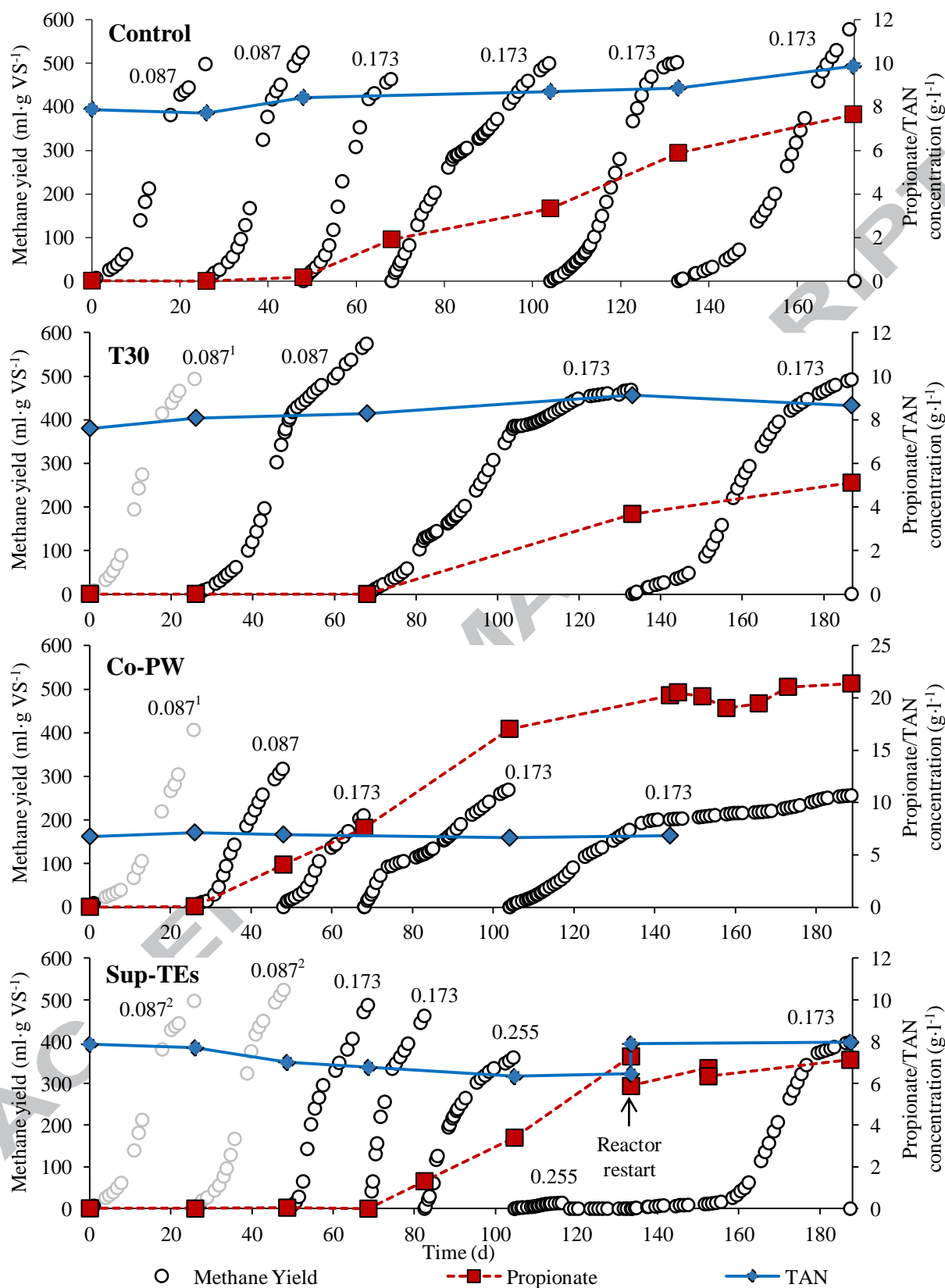


**Figure 1.** Kinetics of methane production in the pilot reactors. The concentrations of propionic acid and TAN after each feeding cycle are also presented. The acetic acid concentrations are shown in Table 5. The numbers on the top of the methane curves stand for the loads applied for each batch ( $\text{kg FW} \cdot \text{kg inoculum}^{-1}$ ). The grey-shaded methane curves

correspond to conditions equivalent to those in the Control reactor (1) and to the results of the Control reactor (2)

ACCEPTED MANUSCRIPT

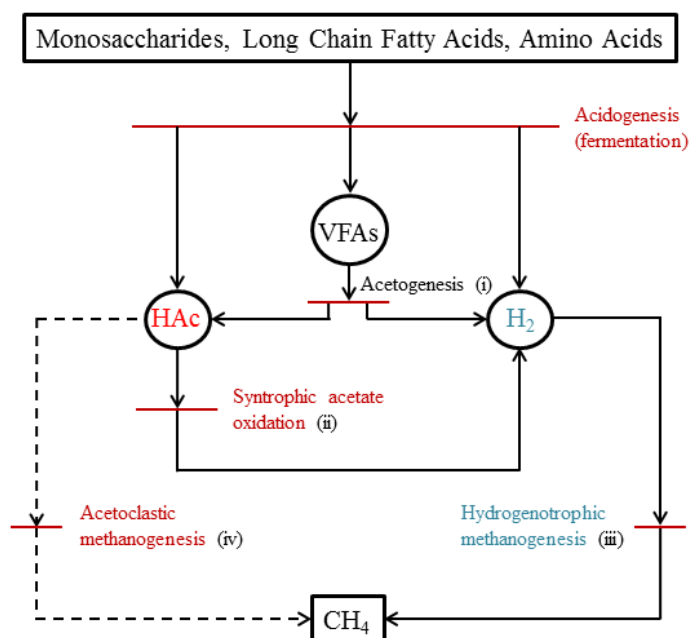


**Figure 2.** Different pathways involved in methane production during AD. The dashed lines represent the pathway inhibited at the high TAN/FAN concentrations associated with FW AD. The main reactions hypothesized to occur during FW AD are shown

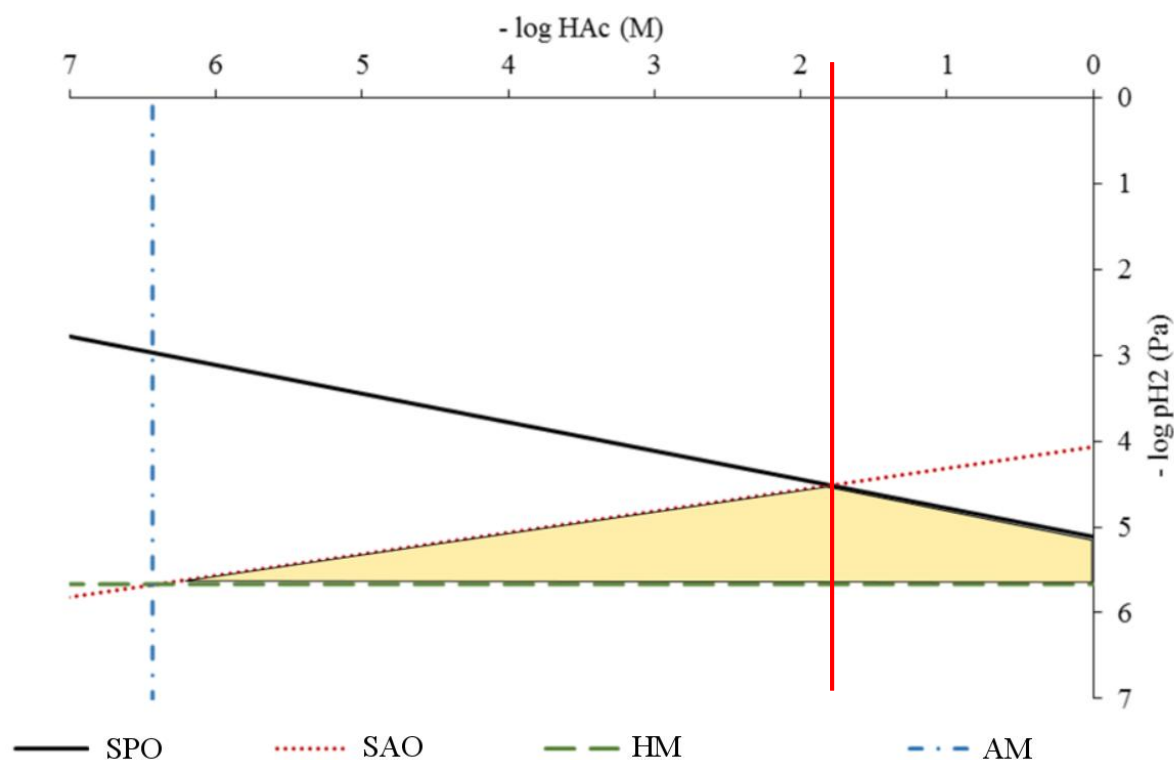


**Figure 3.** Lines of zero  $\Delta G'$  for the reactions shown in Figure 2 at different acetate concentrations and hydrogen partial pressures. They were calculated assuming 298 K, pH 7, 1 mM HPr and 0.1 M  $\text{HCO}_3^-$ . The  $\Delta G^0$  were taken from Zeeman (2005). SPO, SAO, HM and AM stand for syntrophic propionate oxidation, syntrophic acetate oxidation, hydrogenotrophic methanogenesis and acetoclastic methanogenesis, respectively

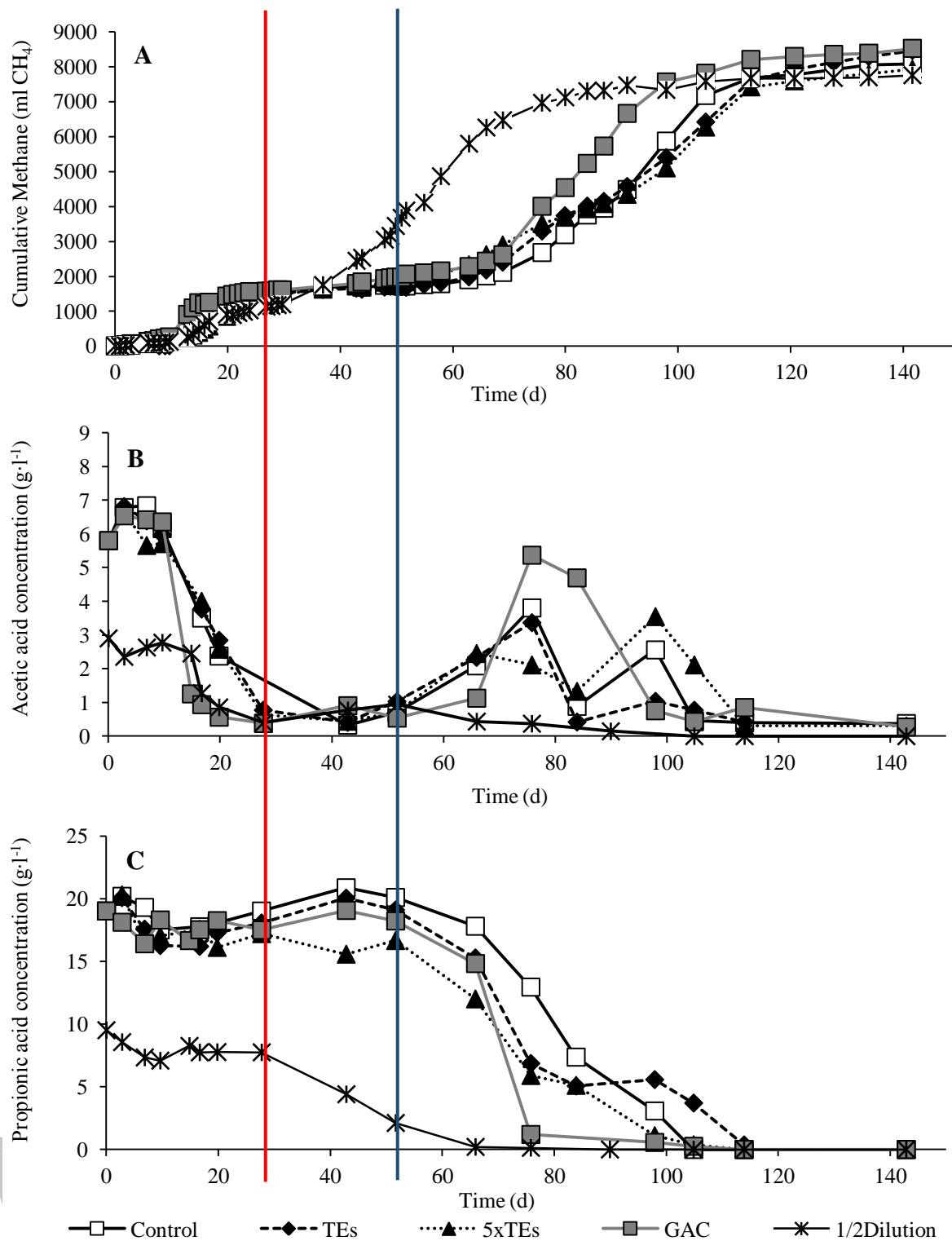


**Figure 4.** Cumulative methane productions (A) and concentrations of acetic acid (B) and propionic acid (C) during the batch experiments. The reactors were incubated at 37 °C for a period of 142 days